ARR No. 4B19

NATIONAL ADVISORY COMMITTEE FOR AERONAUTICS

WARTIME REPORT

ORIGINALLY ISSUED

February 1944 as
Advance Restricted Report 4B19

GENERAL RESISTANCE TESTS ON FLYING-BOAT HULL MODELS

By F. W. S. Locke, Jr.
Stevens Institute of Technology

NACA

WASHINGTON

NATIONAL ADVISORY COMMITTEE FOR AERONAUTICS

ADVANCE RESTRICTED REPORT

GENERAL RESISTANCE TESTS ON FLYING-BOAT HULL MODELS

By F. W. S. Locke, Jr.

SUMMARY

This report re-examines known procedures for handling "general" resistance testing on flying-boat hull models, with particular reference to saving testing time and to improving the usefulness of results to the designer.

It is concluded that the following relationships for collapsing the data from general resistance tests will provide satisfactory accuracy for all loads within practicable limits and that their use permits a considerable reduction in the number of tests required, besides presenting the results in a simple form for ready use:

1. For the displacement range of speeds, using free-to-trim tests with the longitudinal center of gravity located to provide proper trim in the planing range,

$$\frac{C_R}{C_\Delta{}^{2/3}\ C_V{}^2} = \Phi\left(\frac{C_V{}^2}{C_\Delta{}^{1/3}}\right)$$

2. For the planing range of speeds, using fixed-trim tests and making trim angle a parameter,

$$\sqrt{C_R}/C_V = \Phi\ (\sqrt{C_\Delta}/C_V)$$

Figure 8 shows the application of these relationships to a large number of resistance tests made at the Stevens Experimental Towing Tank over a period of time on various models of the XPB2M-1 flying boat. Figure 8a shows satisfactory correlation of the data for the displacement range except in one region. However, in this region the pronounced effect of displacement is of considerable importance to the designer and is forcibly called to his attention. Figure 8b shows contours for the planing range of $\sqrt{C_R}/C_V$ (cross-plotted from an auxiliary chart

not shown) laid onto a grid of trim angle against $\sqrt{C_\Delta}/C_V$. This figure shows porpoising and moment characteristics, as well as resistance characteristics, and thus presents a comprehensive picture of the performance of the hull in the planing range. The relation of a sample "specific" resistance curve to this figure is illustrated by the auxiliary chart (fig. 7).

It is believed that charts of these types are inherently more useful to the designer than the multiplicity of charts ordinarily employed in reporting general resistance tests. By judicious selection of test points, they can be prepared in much less time.

INTRODUCTION

Tank tests of flying-boat hull models, for whatever purpose, are necessarily carried out by one of two methods, the "specific" or the "general" method.

The "specific" method of testing is the more common and usually the quicker to perform. Under this method the water-borne load is made to correspond to a particular function of the speed, or possibly of both the speed and the trim angle. It is frequently found, however, that specific tank tests are not directly applicable even to the actual flying boat for which they were originally intended, because of subsequent modifications to the aerodynamic structure or to the gross weight, which alter the relation of water-borne load to speed. Further, specific tests of older designs, which might otherwise be useful in the preliminary stages of a new design, may be found to be inapplicable because they were made under loading conditions differing from those imposed by the new design.

The "general" method of tank testing effectively avoids these limitations of the specific method by extending the tests to cover wide ranges of combinations of speed, load, and trim. The results are ordinarily presented in an appropriate series of charts from which the designer can select the information needed. The only objections to this method are: (1) that it is time-consuming, both for the testing establishment, in getting sufficiently complete data to cover all the combinations

of conditions which might be required, and for the designer, in deducing answers from the large accumulation of data, and (2) that the multiplicity of charts which must necessarily be consulted complicates considerably the problem of establishing the relative merits of different designs for a particular purpose. These are important objections, however, especially under the stress of war, when time counts heavily.

What is needed is a simplification of the general method which will save time for both the testing establishment and the designer and yet give wholly adequate information. A simplification of the sort required has recently been worked out for porpoising data. (See references 1 and 2.) Here the stability-limit curves for a given hull, obtained from either specific or general tests under various combinations of loading conditions and speed, are collapsed to form a single curve for each of the limits (upper and lower). Parallel simplifications for resistance data have, in fact, been available for some years. It is pointed out in references 3, 4, and 5, for instance, that the data from general resistance tests can be condensed into fewer charts than are ordinarily employed. The suggested procedures have not been widely used, however, possibly because of a feeling that they are good only for first approximations.

A primary purpose of this report is to show, by applying them to actual test data, that certain of these procedures are good for very much more than first approximations and that they can be used with confidence, apart from all questions of time-saving. Their great advantage, as in most cases where data are collapsed into composite curves, is their ability to bring out clear distinctions between accidental and systematic departures from the composite curves. This is vividly illustrated in the chart for the displacement range of the XPB2M-1 (fig. 8a), where the discontinuities focus attention on a point of interest which might easily have been overlooked in plots of the ordinary sort.

It is shown in this report, in particular, that for most practical purposes the results of general resistance tests can be condensed into two charts, one for free-to-trim resistances and trim angles in the displacement range of speeds, the other for resistances in the planing range of speeds. The latter chart is

given the same form as the chart employed in references 1 and 2 for presenting the results of general porpoising tests; it can therefore be used to show, in addition to the resistance characteristics, the dynamic stability and the moment characteristics of the hull in the planing range.

Only a few special tests were made for this report. Published data, or tests already on hand, were used for most of the analyses.

This investigation, conducted at the Stevens Institute of Technology, was sponsored by, and conducted with financial assistance from, the National Advisory Committee for Aeronautics.

ANALYSIS

In starting from rest and taking off the water, the hull of a flying boat passes through two more or less distinct speed ranges. These are the displacement range, covering roughly the lower half of the complete speed range to take-off, and the planing range, covering the upper half. It is necessary to consider the two ranges separately; actually, of course, they merge smoothly from one to the other.

(a) Displacement Range

In the displacement range, resistance arises mainly from skin friction and wave-making. Hence the ordinary relationship used for handling surface-vessel resistances would be expected to apply where geometric similarity exists. This, in non-dimensional form, is

$$\frac{R}{\lambda^2 \rho/2 \, v^2} = \Phi \left(\frac{v^2}{g\lambda}, \frac{v\lambda}{\nu} \right) \qquad (1)$$

where

R resistance

ρ mass density

v speed

g gravity acceleration

ν kinematic viscosity

Φ function

and

$\frac{v^2}{g\lambda}$ Froude number

$\frac{v\lambda}{\nu}$ Reynolds number

λ linear dimension, not yet specified, which defines size

But it is common practice in dealing with flying-boat hulls to disregard the variation of the skin friction coefficient with the Reynolds number; no very new assumption is therefore involved when equation (1) is simplified by omitting the Reynolds number, making it

$$\frac{R}{\lambda^2 \rho/2 \, v^2} = \Phi\left(\frac{v^2}{g\lambda}\right) \qquad (2)$$

Equation (2) may be presumed satisfactory, then, for collapsing the data for geometrically similar flying-boat hulls under similar loading. And this will be equally true whatever linear dimension is selected for λ.

The usefulness of a relationship for the purpose in hand depends, however, not upon its success in collapsing the data for geometrically similar cases of differing size (which is only the first requirement), but upon its success in collapsing the data for cases which are not geometrically similar. Perring showed, in reference 3, that in one instance the same relationship served this broader purpose quite well, provided $(\text{Vol})^{1/3}$ was used for λ, making

$$\frac{R}{(\text{Vol})^{2/3} \rho/2 \, v^2} = \Phi\left(\frac{v^2}{g\,(\text{Vol})^{1/3}}\right) \qquad (3)$$

where

(Vol) submerged volume corresponding to the water-borne load: namely, Δ/w

Δ water-borne load

and

w specific weight of water

or, substituting the usual NACA coefficients,

$$\frac{C_R}{C_\Delta^{2/3}\ C_V^2} = \phi\left(\frac{C_V^2}{C_\Delta^{1/3}}\right) \qquad (4)$$

The transformation from equation (3) to equation (4) is given here in its entirety to avoid any possible question regarding the use of "beam" as a factor. It will be seen that this factor appears only as an arbitrary reference length to define coefficients; it is not used to define size.

By definition,

$$C_R = \frac{R}{w\ b^3}$$

$$C_\Delta = \frac{\Delta}{w\ b^3}$$

$$C_V = \frac{V}{\sqrt{g\ b}}$$

$$(Vol) = \frac{\Delta}{w}$$

where b is the beam, whence

$$R = w\ b^3\ C_R$$

$$V^2 = g\ b\ C_V^2$$

$$(Vol) = \frac{w\ b^3\ C_\Delta}{w} = b^3\ C_\Delta$$

Substituting the latter expressions in equation (3), it is seen that

$$\frac{w\ b^3\ C_R}{\beta^2\ C_\Delta^{2/3}\ \rho/2\ g\ b\ C_V^2} = \phi\left(\frac{g\ b\ D_V^2}{g\ b\ C_\Delta^{1/3}}\right)$$

which reduces to

$$\frac{C_R}{C_\Delta^{2/3}\ C_V^2} = \phi\left(\frac{C_V^2}{C_\Delta^{1/3}}\right) \qquad (4)$$

Departures from geometric similarity may be introduced by changing any of the three variables

1. Hull form
2. Water-borne load
3. Trim

and there is no particular reason for assuming, a priori, that any one of the three is necessarily more significant than any other. However, since comparisons will ordinarily be desired between different hull forms, attention may usually be concentrated on the other two variables.

The charts comprising figure 2 show, accordingly, the application of equation (4) to a series of low-speed resistance tests on a <u>particular model</u>, representing the Sikorsky S-40 flying-boat hull. The tests were made by the NACA and are reported in reference 6. Three of the charts show the results for various loads at three different values of <u>fixed trim</u> (making load the only variable), while the fourth chart shows the mean lines from the other three. It will be seen that, for the ranges covered, the effects of load variation have been quite successfully collapsed into a single curve and the effects of trim variation a little less successfully collapsed. But this apparent difference in the relative success with which load and trim variations are collapsed is of less significance than it may appear at first sight. While the range of load

variation covered is an entirely reasonable one, the range of trim variation, from 5° to 9°, is unreasonably large when applied to all speeds within the displacement range. This trim range, while easily obtained in model tests by fixing trims, would involve such large applied moments that its occurrence in full size would be most unlikely – particularly since the longitudinal position of the center of gravity, which is the most powerful factor affecting the resultant applied moment at displacement speeds, must ordinarily be fixed within relatively narrow limits by considerations of trim in the planing range.

The upper chart of figure 8 shows results for another model, representing the XPB2M-1 flying boat, deduced from tests made at the Experimental Towing Tank and for this report. In this case, however, free-to-trim data, instead of fixed-trim data, were used, and the longitudinal position of the center of gravity was reasonably suitable from the point of view of trim in the planing range. It will be seen that, apart from a region in the middle of the range ($C_V^2/C_\Delta^{1/3}$ = 5.0 to 8.0), where large discrepancies occur, the data are very successfully collapsed into a single curve. This middle range was mentioned under Summary and is shown later to mark a very pronounced variation in performance with variation in loading; hence the fact that the chart causes it to stand out vividly will be seen to add to rather than detract from an estimate of the value of the relationship under consideration.

It may be concluded, then, that the relationship expressed by equation (4), in combination with free-to-trim data taken with a suitable longitudinal position of the center of gravity, is a useful means of condensing the results of general resistance tests in the range of displacement speeds.

(b) Planing Range

It would be expected that, as the speed increases beyond the displacement range and true planing begins, the Froude number would become less and less important. Thus the basic relationship

$$\frac{R}{\lambda^2 \ \rho/2 \ v^2} = \Phi \left(\frac{v^2}{g\lambda}\right) \qquad (2)$$

would be expected to give way to the simpler relationship

$$\frac{R}{\lambda^2 \ \rho/2 \ v^2} = K \qquad (5)$$

in cases of geometric similarity, and apart from the definition of λ.

That this expection is borne out by the facts is shown in figure 1, which is actually one of the charts of figure 2 extended into the planing range. Here the horizontal line for any one load indicates that $\frac{C_R}{C_\Delta^{2/3} \ C_V^2}$ has become independent of $\frac{\partial V^2}{C_\Delta^{1/3}}$, which means that $\frac{R}{(Vol)^{2/3} \ \rho/2 \ v^2}$ has become independent of the Froude number. But this chart indicates, in addition, that even with the trim angle fixed, the expression

$$\frac{R}{(Vol)^{2/3} \ \rho/2 \ v^2} = K \qquad (6)$$

which is related to equation (5) in the same way that equation (3) is related to equation (2), does not completely collapse the data for variations of load. Thus it is clear that a simple extension of the displacement-range relationship will not suffice for the planing range.

The displacement-range relationship fails in the planing range primarily because the definition

$$(Vol) = \Delta/w$$

which is the foundation of equation (3), no longer holds when, in the planing range, dynamic lifting force predominates.

A simple basic relationship for the planing range is

$$R = \Phi(\Delta) \tag{7}$$

or, in non-dimensional form

$$\frac{R}{\lambda^2 \rho/2 v^2} = \Phi \frac{\Delta}{\lambda^2 \rho/2 v^2} \tag{8}$$

where Δ is, as before, the water-borne load and the definition of λ is immaterial, or again substituting the usual NACA coefficients,

$$\frac{C_R}{C_V^2} = \Phi\left(\frac{C_\Delta}{C_V^2}\right) \tag{9}$$

$$\frac{\sqrt{C_R}}{C_V} = \Phi\left(\frac{\sqrt{C_\Delta}}{C_V}\right) \tag{9}'$$

The transformation from equation (8) to (9) corresponds to the transformation from equation (3) to (4).

References 3, 4, 5, and 7, show that this basic relationship, in one form or another, has been used with good success in the past for collapsing resistance data in the planing range. The relationship is here tested by applying it to fixed-trim data in the planing range, for one of the models considered in the displacement-range analysis above,

The Sikorsky S-40 model (data from reference 6). (See figs. 3 and 4.)

and to similar data for

A simple V-bottom planing surface (data from reference 8) (See figs. 5 and 6.)

The square root form, equation (9)' is used for plotting, and the scale of abscissas is started from the right. This is consistent with the procedure adopted in references 1 and 2 for porpoising data; it avoids some distortion of the curves and puts the take-off ($\sqrt{C_\Delta}/C_V = 0$) at the right of the sheet.

It will be seen that in all cases the data for fixed values of trim are very satisfactorily collapsed. There is some variation between the mean curves for the various trim angles of each model, but as trim control is ordinarily available in the planing range (through the elevators), there is no purpose in attempting to to smooth out its effects. Instead, contours of $\sqrt{C_R}/C_V$ have been drawn from the mean curves for fixed trims, on a grid of trim angle against $\sqrt{C_\Delta}/C_V$, making a sheet of exactly the same form suggested in references 1 and 2 for porpoising data.

An additional test of the relationship is given in figure 9, which shows the results at one value of trim for

NACA Model No. 11 (data from reference 9) (See fig. 9.)

This case is included to illustrate that the relationship will bring out a discontinuity clearly, and that it will successfully collapse planing-range data even under such an extreme condition as transferring the entire load to the afterbody.

It may be concluded, then, that the relationship expressed by equation (9) is a satisfactory means of condensing the results of general resistance tests at fixed trims, in the range of planing speeds.

The lower chart of figure 8 shows the contours of $\sqrt{C_R}/C_V$ for the XPB2M-1, prepared from unpublished data gathered at Stevens Institute for The Glenn L. Martin Company, together with the stability limits and the moment data from reference 2.

DISCUSSION

As previously described, the two charts of figure 8 suffice to show all the general resistance data for the particular hull to which they refer, as well as stability limits and moment data in the planing range. The form of plotting of these charts may be more or less unfamiliar, making it difficult to visualize their relation to

more conventional forms of presentation. In an attempt to remedy this, figure 7 has been prepared. It shows a "specific" resistance curve of the ordinary sort, as deduced from the charts of figure 6 for the loading curve (and trim track in the planing range) indicated, which correspond to the normal particulars of the XPB2M-1. Circled numbers, corresponding with circled numbers in figure 6, serve to indicate the connection between the two forms of plotting.

The need for two different relationships, for the two speed ranges, is naturally an inconvenience. It should be especially noted, however, that this need arises, not through any loss of accuracy when the relationship for one speed range is carried over into the other, but simply because the test data are no longer successfully collapsed. Thus nothing more serious than inconvenience can result. The need appears to be inevitable; it is attributable, as previously noted, to the basically different ways in which the water-borne load is supported in the two speed ranges. This is illustrated in the following sketches.

In the displacement range, support is by buoyant forces.

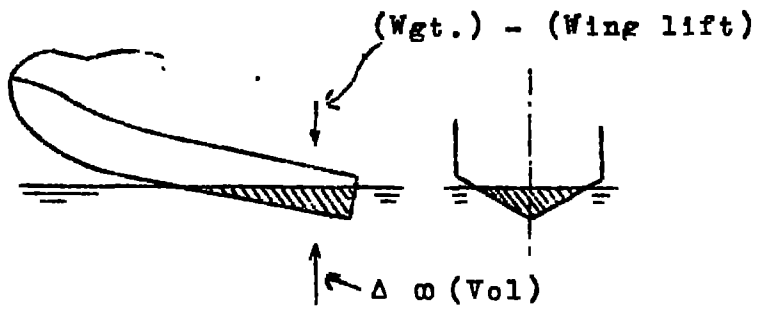

In the planing range, support is by dynamic forces.

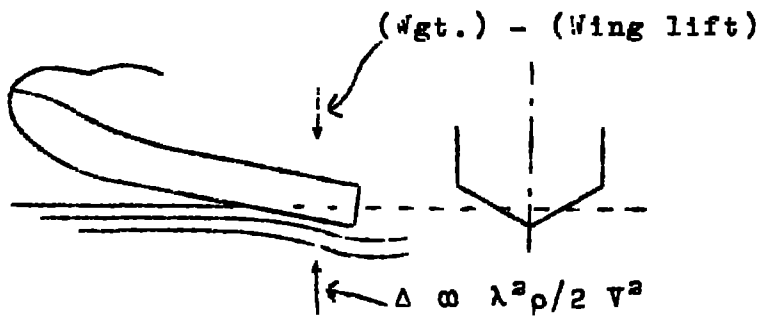

Referring to the planing-range relationship: With fixed trim, a constant value of the "lift coefficient" $\frac{\Delta}{\lambda^2 \, \rho/2 \, v^2}$, or $\sqrt{C_\Delta}/C_V$, apart from the values of the individual factors, would be expected to result in a constant geometric shape. Hence the evidence of all of the planing-range charts here presented, that it results also in a constant value of the resistance coefficient $\frac{R}{\lambda^2 \, \rho/2 \, v^2}$, or $\sqrt{C_R}/C_V$ (which implies a constant flow pattern), is not very surprising.

Referring to the displacement-range relationship: A constant Froude number $\frac{v^2}{g \, (Vol)^{1/3}}$, or $C_V{}^2/C_\Delta{}^{1/3}$, on the other hand, either with or without fixed trim, does not in any sense imply a constant geometric shape. Hence the evidence of the displacement-range charts here presented, that the resistance coefficient $\frac{R}{(Vol)^{2/3} \, \rho/2 \, v^2}$, or $\frac{C_R}{C_\Delta{}^{2/3} \, C_V{}^2}$, is, in general, a function of the Froude number primarily, is less easily explained. In fact, the only possible explanation is that the variations from a single geometric shape introduced with variations of load (or trim) are not large enough to affect appreciably the resistance characteristics. If actual hulls had the simple "wedge" form indicated in the foregoing sketches, there would, of course, be no change of shape with load variation and only moderate changes of shape with normal trim variation. The wedge form is obviously a reasonably good representation of most actual hulls for the planing range. It is a much less obvious choice for the displacement range, but Perring used it as a working hypothesis in developing equation (3) for this range (reference 3), and the success of the displacement-range correlations presented in this report tend to confirm its general reliability for representing actual hulls.

There evidently must be limits, however, beyond which the displacement-range relationship will no longer

collapse data – beyond which the variations from a single geometric shape have become large. With sufficient load, for instance, the bow will plow heavily in the displacement range, or even dive. The relationship may break down, too, under less extreme conditions – the middle region on the displacement–range chart for the XPB2M–1, in figure 8a, being a case in point. Here the discontinuities were observed to originate with wetting of the tail cone and of the afterbody sides near the sternpost, which resulted in discernible differences in the flow pattern with variation of load and corresponding differences in the resistance coefficient. This, however, is precisely the information which needs to be brought to light for the hull in question. Except in this one region, the resistance data are satisfactorily collapsed, indicating consistent performance of the hull throughout the range of loads investigated; within this one region, better performance is obtained with lighter loads. The additional information can be deduced, also, that most of the penalty within the region is incurred in raising the load to about $C_\Delta = 0.90$ and that very little extra penalty is incurred with further increase of load.

The ability of the charts to bring out such characteristics as this is a very important advantage to be gained by condensing the data. From this point of view, failure to collapse completely the data for a given hull is looked upon, not as a weakness of the relationship, but, in truer perspective, as an indication that a significant variation of shape or flow pattern has occurred. The planing–range relationship here proposed is as successful in this respect as the displacement–range relationship; a variation caused by increase of load will be shown, for instance, by an up–sweep of the curve of $\sqrt{C_R}/C_V$ against $\sqrt{C_\Delta}/C_V$ as high values of $\sqrt{C_\Delta}/C_V$ are approached.

In appraising this advantage, however, the basic purpose of condensing the data should not be lost sight of: namely, that the testing time can be reduced and the results made more readily useful to the designer. The advantage just described is essentially an extension of this basic purpose. Care must be taken, too, to avoid attaching importance to indicated variations which are, in fact, caused only by the relationship in question

having been pushed too far in the direction of the opposite speed range. Such variations may be encountered at the upper end of curves for the displacement-range relationship or at the lower end of curves for the planing-range relationship, as indicated on various of the charts. They are otherwise of minor importance, being primarily an inconvenience. In general, the curves for the two speed ranges should be extended so that they overlap.

A good example of the usefulness of combining resistance and porpoising data in one chart is presented by the planing-range chart for the XPB2M-1 (fig. 8b). Here it will be seen that the resistance data extend a long way into the range of unstable trim angles, showing that a good many unnecessary data were obtained in the general resistance tests. If the resistance tests had been made after, or, better still, in conjunction with, the porpoising tests, it is clear that time could have been saved or more complete information obtained for the useful range.

A study of the scatter of the test points on the various charts indicates satisfactory accuracy wherever the relationships may be expected to apply. The scatter of points is somewhat greater in the displacement range, as compared with the planing range. This probably is due to the greater likelihood of systematic departures attributable to variations of shape, rather than to greater experimental errors in this range. In both ranges, the mean curves ordinarily will be better than the mean curves drawn in conventional charts by virtue of the greater number of tests points on which they are based.

This last suggests that the methods constitute a useful means of fairing data, even though the data are eventually reported on more conventional charts.

CONCLUDING REMARKS

In considering means for condensing the data from "general" resistance tests, it is not supposed that use of these means, or even of the method of general resistance testing itself, will ever completely eliminate the need for "specific" tests and test reports. So much is at stake in the development of a large modern flying boat that specific tests, particularly in the later stages of designing, will undoubtedly be needed for some time to come.

It is believed, however, that the particular procedures presented for condensing resistance data should be a definite help to the designer, both by facilitating critical comparisons between different hull designs, and by presenting the data in a convenient form for ready reference in studies of take-off performance. They are of advantage to the testing establishment because, by carefully selecting test points, the same ground ordinarily covered in general resistance testing may be explored in less time.

Experimental Towing Tank,
Stevens Institute of Technology,
Hoboken, N.J., June 5, 1943.

REFERENCES

1. Locke, F. W. S., Jr.: General Porpoising Tests on Flying-Boat-Hull Models. NACA ARR No. 3I17, Sept. 1943.

2. Davidson, Kenneth S. M., and Locke, F. W. S., Jr.: Some Analyses of Systematic Experiments on the Resistance and Porpoising Characteristics of Flying-Boat Hulls. NACA ARR No. 3I06, Sept. 1943.

3. Perring, W. G. A.: Water Performance of Seaplanes. Tank Data to Determine Effect of Wind, Variation of Loading or a Change of Air Structure. R. & M. No. 1657, British A.R.C., 1935.

4. Perring, W. G. A., and Johnston, L.: Hydrodynamic Forces and Moments on a Simple Planing Surface and on a Flying Boat Hull. R. & M. No. 1646, British A.R.C., 1935.

5. Schroeder, P.: The Take-Off of Seaplanes, Based on a New Hydrodynamic Reduction Theory. T.M. No. 621, NACA, 1931.

6. Dawson, J. R.: A Complete Tank Test of the Sikorsky S—40 Flying Boat — American Clipper Class. T.N. No. 512, NACA, 1934.

7. Locke, F. W. S.: A Comparison of Stevens and N.A.C.A. Tests in the Planing Range of the Navy Mark V Seaplane Hull. Stevens Experimental Towing Tank Technical Memorandum No. 47, 1940.

8. Shoemaker, J. M.: Tank Tests of Flat and V—Bottom Planing Surfaces. T.N. No. 509, NACA, 1934.

9. Shoemaker, J. M., and Parkinson, J. B.: A Complete Tank Test of a Model of a Flying—Boat Hull — N.A.C.A. Model No. 11. T.N. No. 464, NACA, 1933.

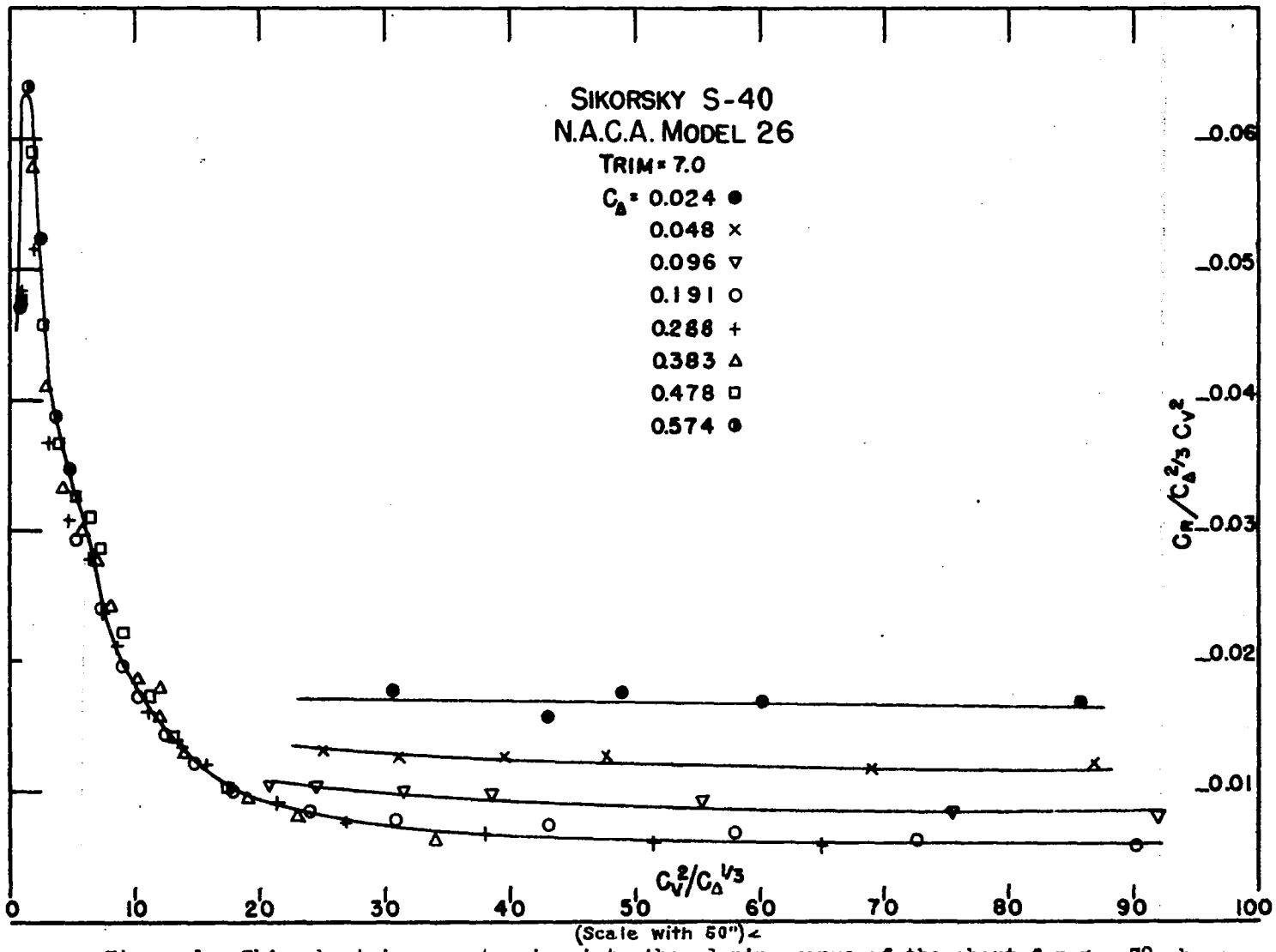

Figure 1. This chart is an extension into the planing range of the chart for $\tau = 7^\circ$ shown on the opposite page. Its purpose is to show that the displacement-range relationship will not completely collapse data in the planing range. Data for lower values of C_Δ than those that appear on the opposite page are included to emphasize this.

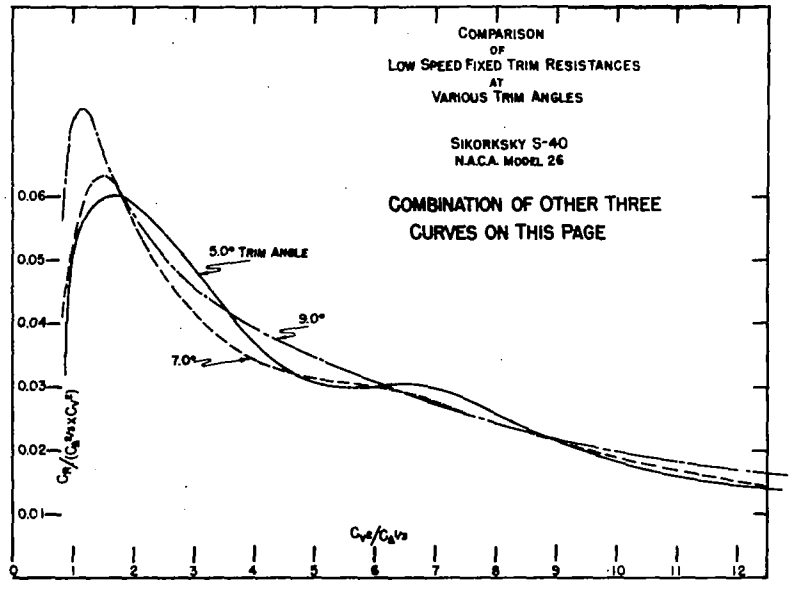

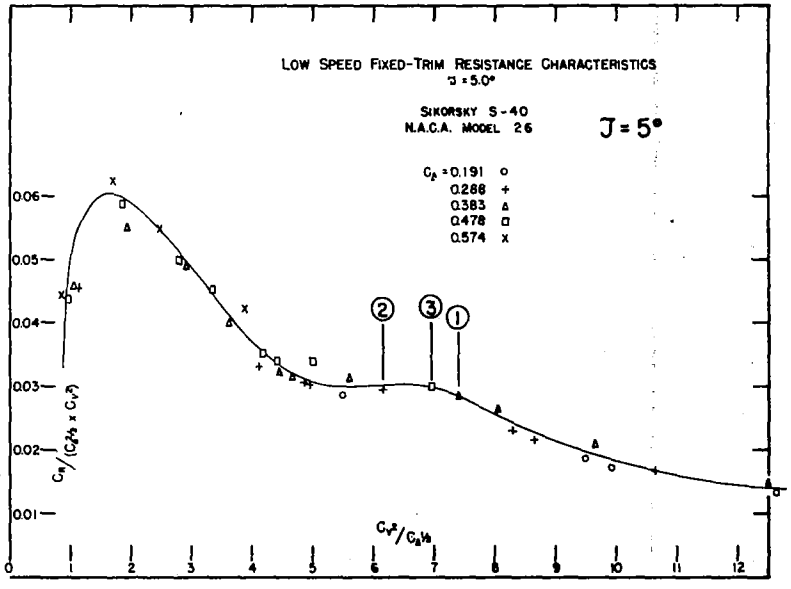

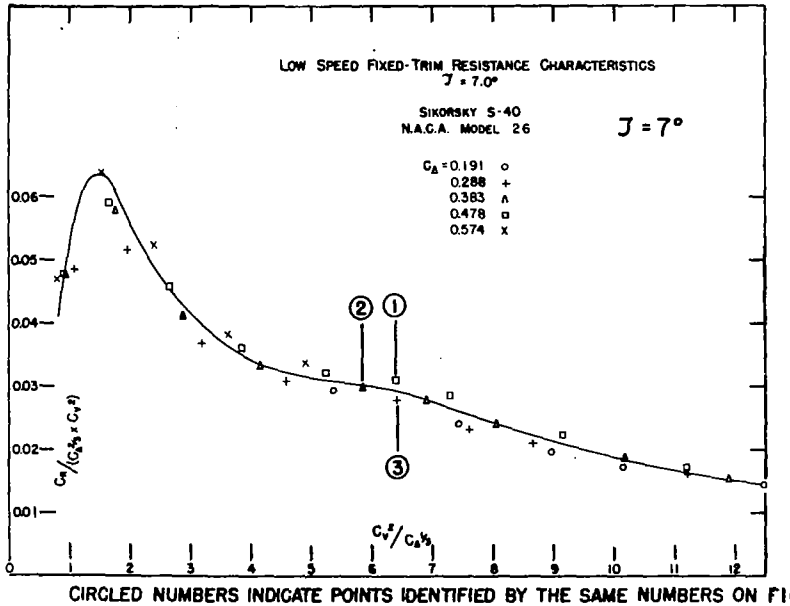

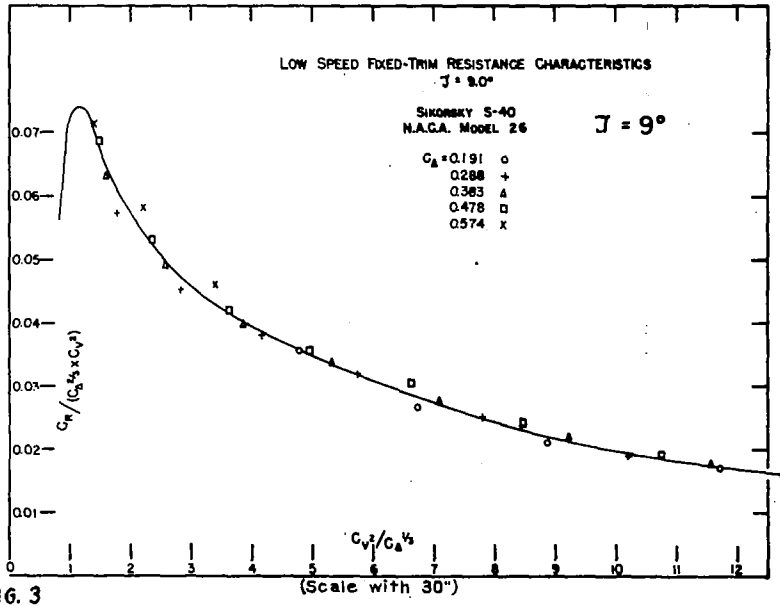

CIRCLED NUMBERS INDICATE POINTS IDENTIFIED BY THE SAME NUMBERS ON FIG. 3

(Scale with 30")

NACA

Fig. 2

CIRCLED NUMBERS INDICATE POINTS IDENTIFIED BY THE SAME NUMBERS ON FIG. 2

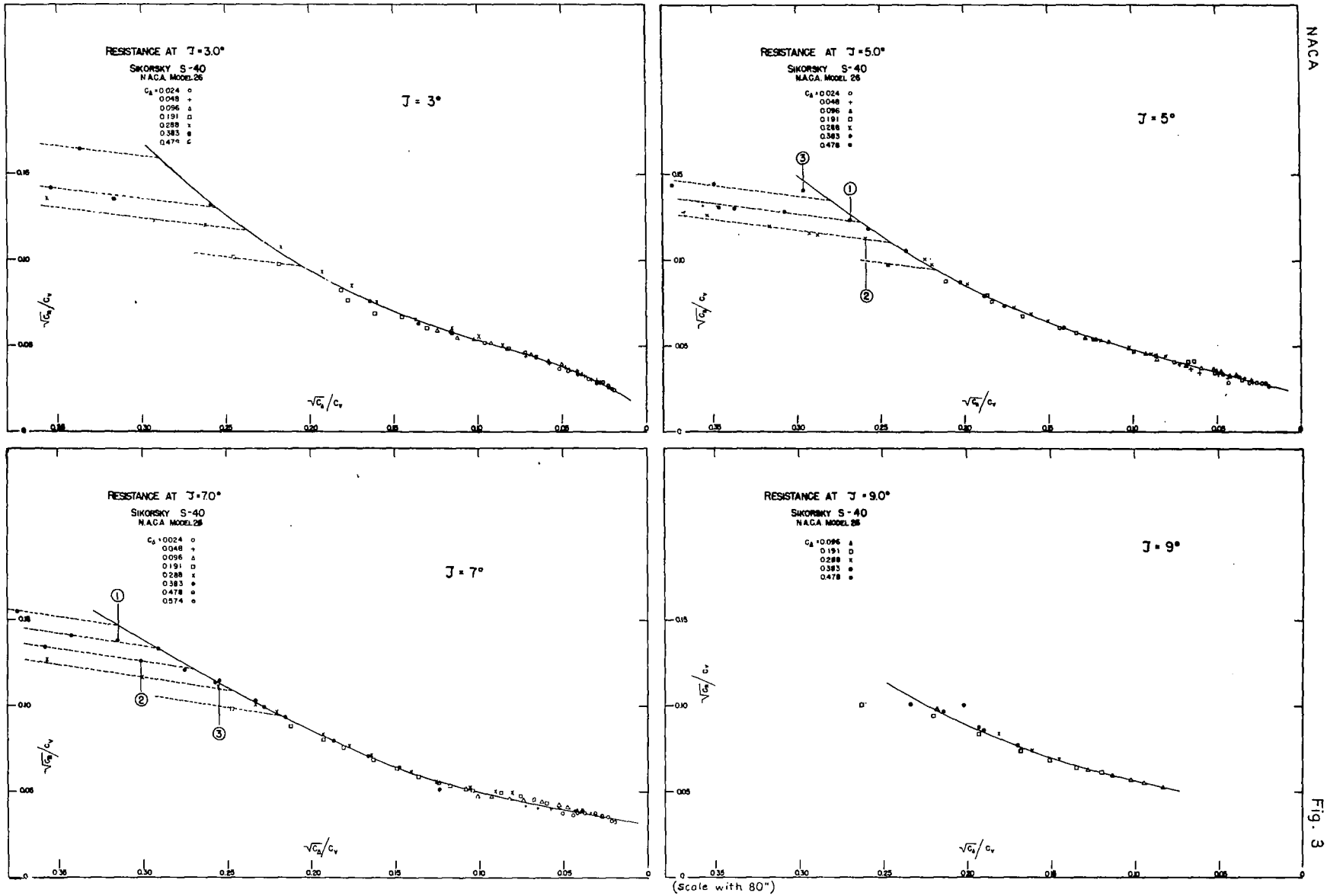

(Scale with 80")

NACA

Fig. 3

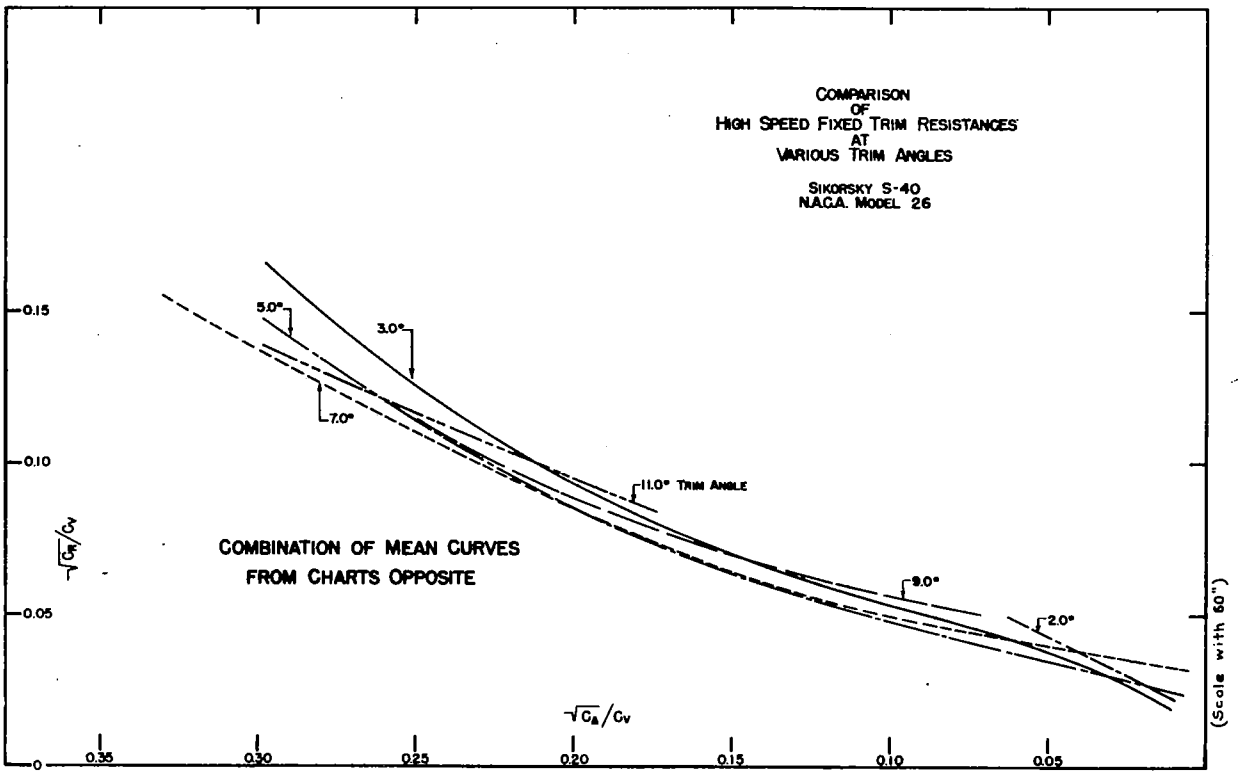
COMPARISON
OF
HIGH SPEED FIXED TRIM RESISTANCES
AT
VARIOUS TRIM ANGLES
SIKORSKY S-40
N.A.C.A. MODEL 26
5.0°
3.0°
7.0°
11.0° TRIM ANGLE
9.0°
2.0°
COMBINATION OF MEAN CURVES
FROM CHARTS OPPOSITE
$\sqrt{C_R}/C_V$
$\sqrt{C_\Delta}/C_V$
0.35
0.30
0.25
0.20
0.15
0.10
0.05
0
(Scale with 60")

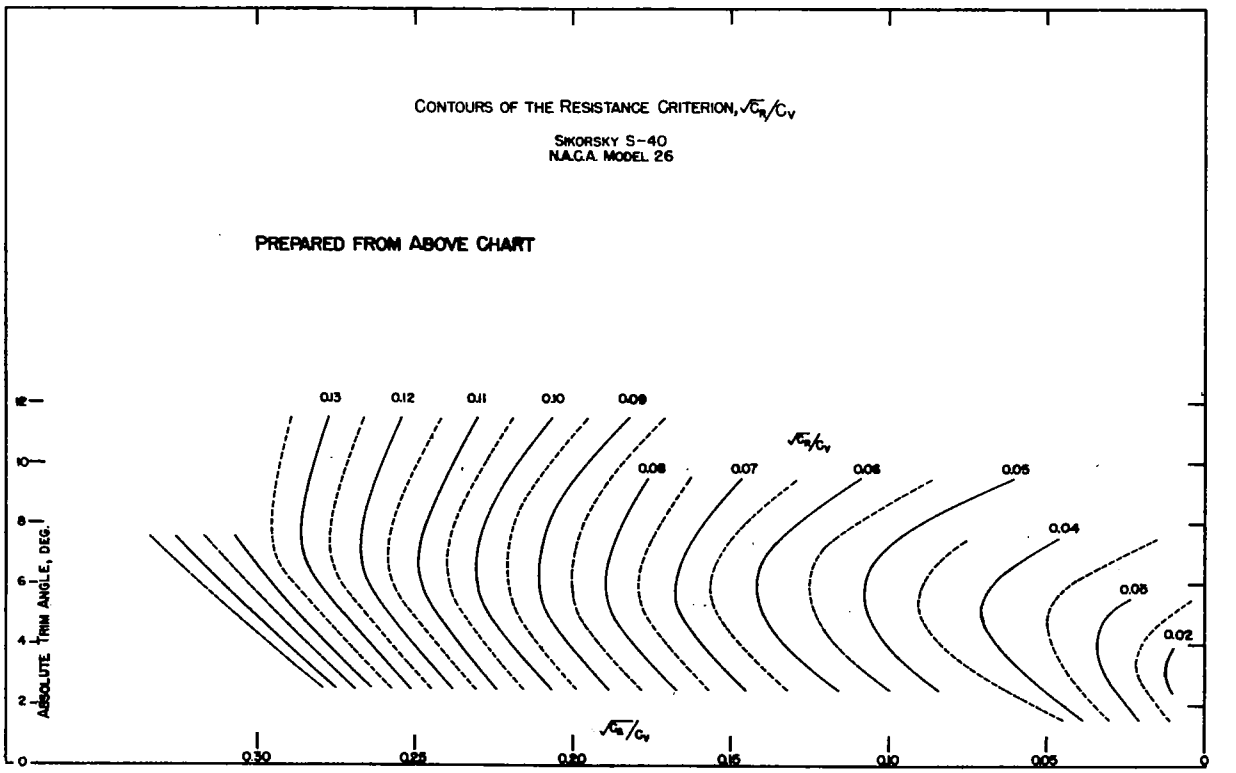
CONTOURS OF THE RESISTANCE CRITERION, $\sqrt{C_R}/C_V$
SIKORSKY S-40
N.A.C.A. MODEL 26
PREPARED FROM ABOVE CHART
ABSOLUTE TRIM ANGLE, DEG.
0.13
0.12
0.11
0.10
0.09
0.08
0.07
0.06
0.05
0.04
0.03
0.02
$\sqrt{C_R}/C_V$
$\sqrt{C_\Delta}/C_V$
0.30
0.25
0.20
0.15
0.10
0.05
0

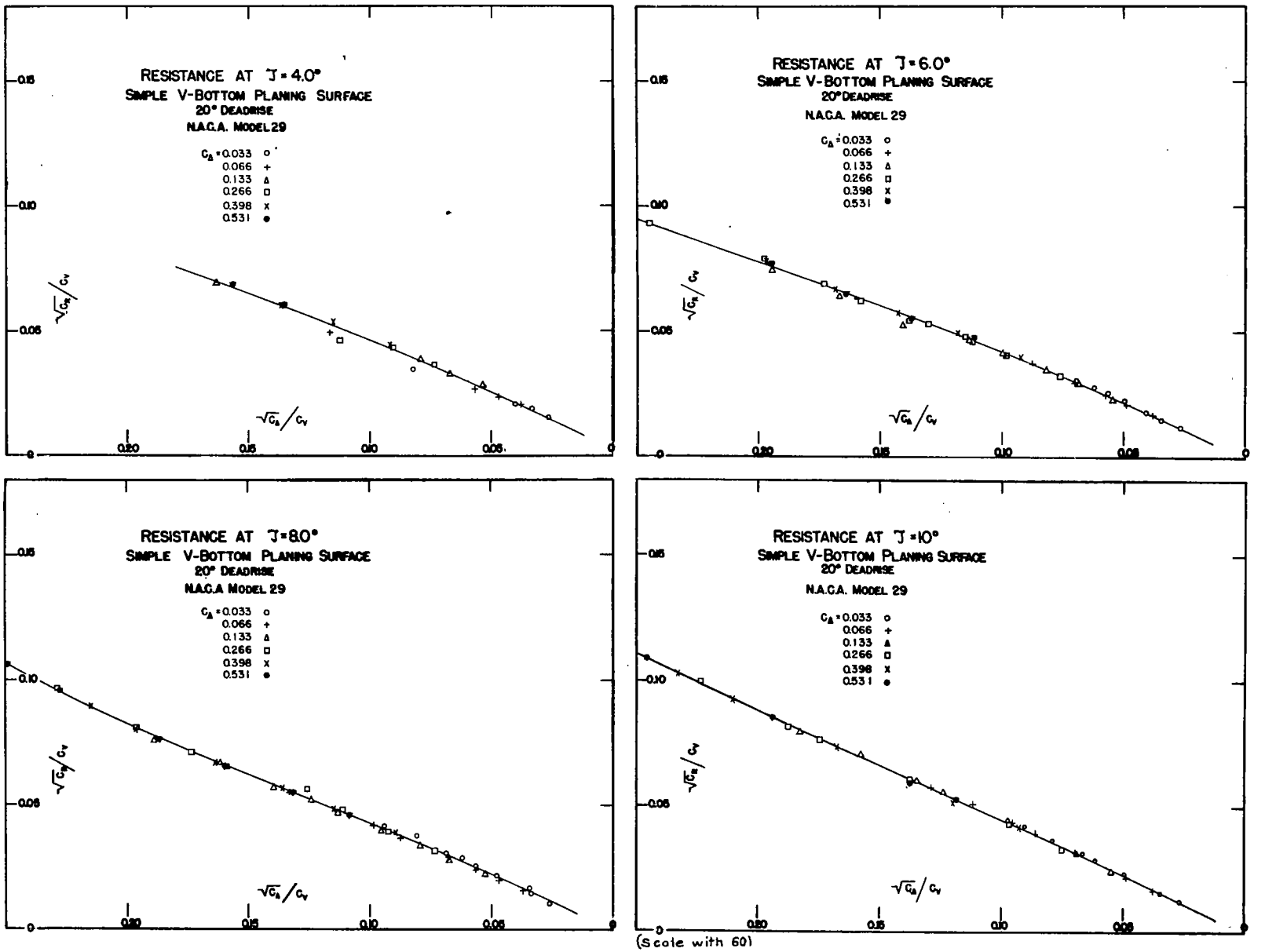
RESISTANCE AT τ = 4.0°
SIMPLE V-BOTTOM PLANING SURFACE
20° DEADRISE
N.A.C.A. MODEL 29
C_Δ = 0.033 o
0.066 +
0.133 Δ
0.266 □
0.398 x
0.531 ●
$\sqrt{C_R}/C_V$
$\sqrt{C_\Delta}/C_V$
RESISTANCE AT τ = 6.0°
SIMPLE V-BOTTOM PLANING SURFACE
20° DEADRISE
N.A.C.A. MODEL 29
C_Δ = 0.033 o
0.066 +
0.133 Δ
0.266 □
0.398 x
0.531 ●
$\sqrt{C_R}/C_V$
$\sqrt{C_\Delta}/C_V$
RESISTANCE AT τ = 8.0°
SIMPLE V-BOTTOM PLANING SURFACE
20° DEADRISE
N.A.C.A MODEL 29
C_Δ = 0.033 o
0.066 +
0.133 Δ
0.266 □
0.398 x
0.531 ●
$\sqrt{C_R}/C_V$
$\sqrt{C_\Delta}/C_V$
RESISTANCE AT τ = 10°
SIMPLE V-BOTTOM PLANING SURFACE
20° DEADRISE
N.A.C.A. MODEL 29
C_Δ = 0.033 o
0.066 +
0.133 Δ
0.266 □
0.398 x
0.531 ●
$\sqrt{C_R}/C_V$
$\sqrt{C_\Delta}/C_V$
(Scale with 60)

Fig. 5

NACA

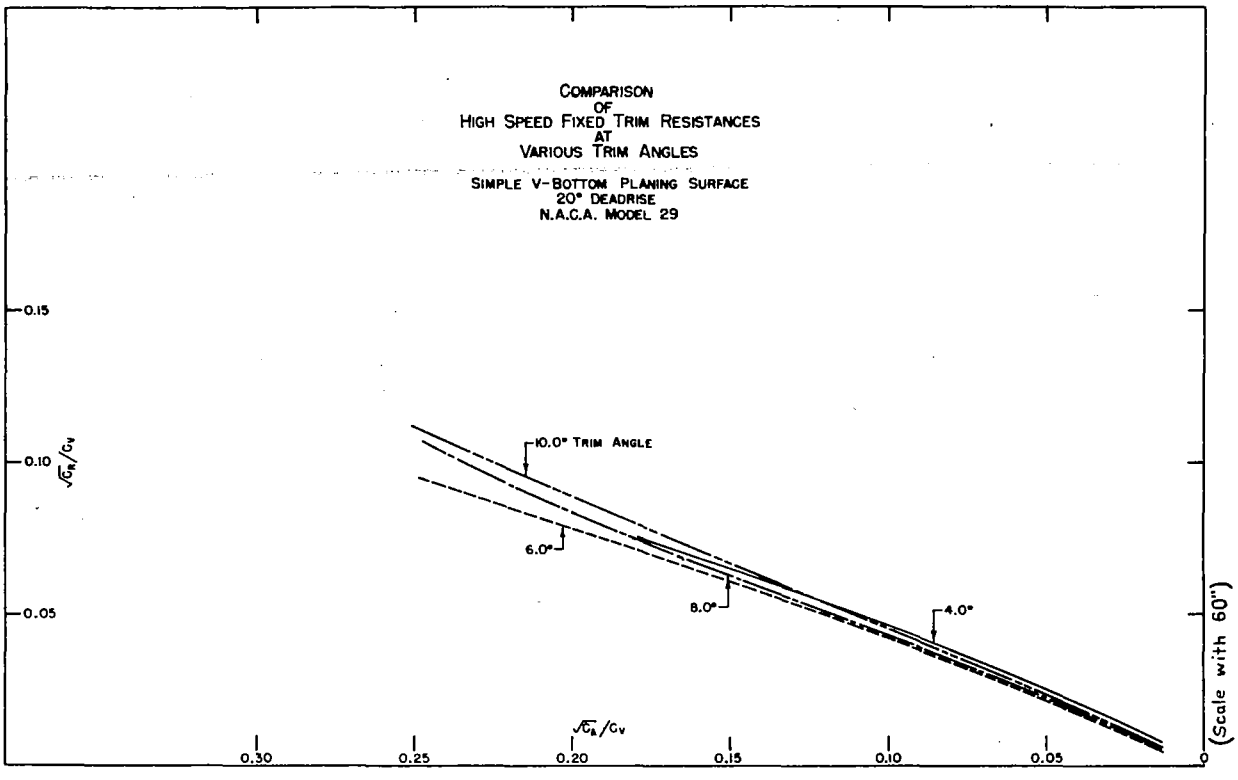
COMPARISON
OF
HIGH SPEED FIXED TRIM RESISTANCES
AT
VARIOUS TRIM ANGLES
SIMPLE V-BOTTOM PLANING SURFACE
20° DEADRISE
N.A.C.A. MODEL 29
0.15
0.10
0.05
$\sqrt{C_R}/C_V$
10.0° TRIM ANGLE
6.0°
8.0°
4.0°
$\sqrt{C_\Delta}/C_V$
0.30
0.25
0.20
0.15
0.10
0.05
0
(Scale with 60")

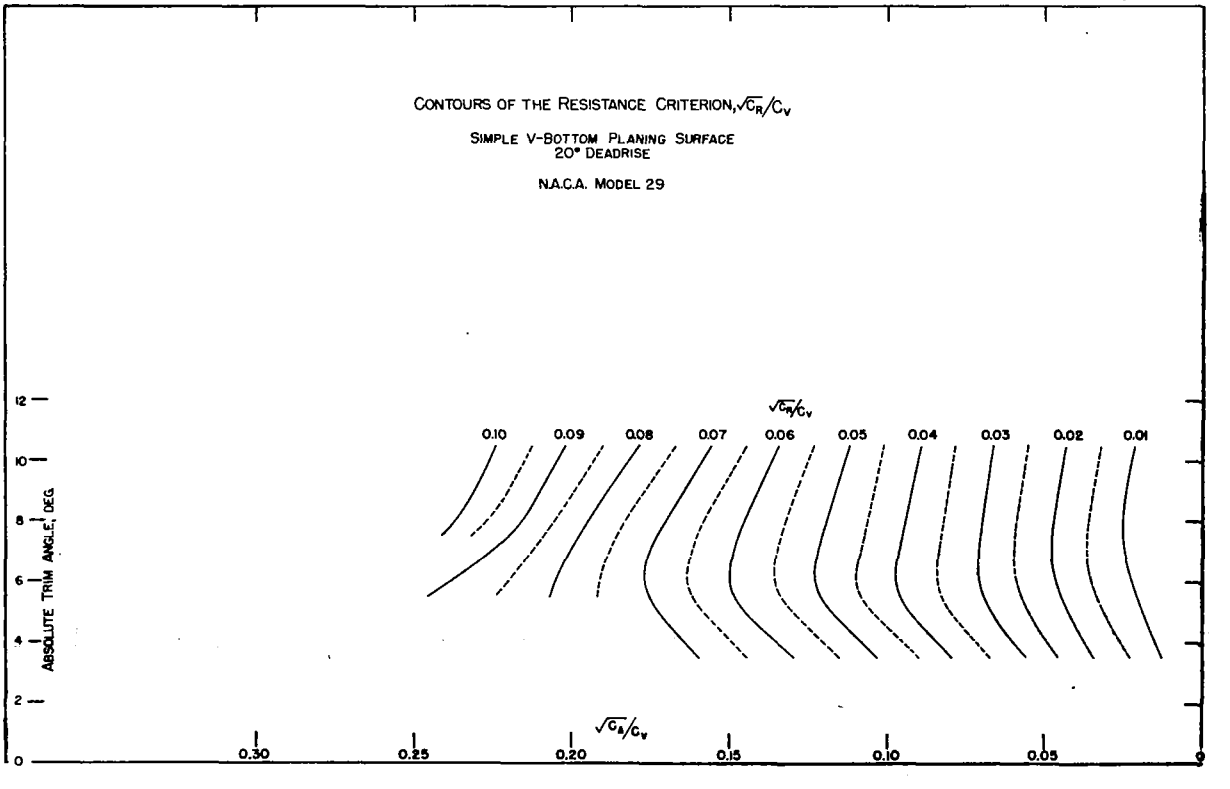
CONTOURS OF THE RESISTANCE CRITERION, $\sqrt{C_R}/C_V$
SIMPLE V-BOTTOM PLANING SURFACE
20° DEADRISE
N.A.C.A. MODEL 29
ABSOLUTE TRIM ANGLE, DEG.
12
10
8
6
4
2
0
$\sqrt{C_R}/C_V$
0.10
0.09
0.08
0.07
0.06
0.05
0.04
0.03
0.02
0.01
$\sqrt{C_\Delta}/C_V$
0.30
0.25
0.20
0.15
0.10
0.05
0

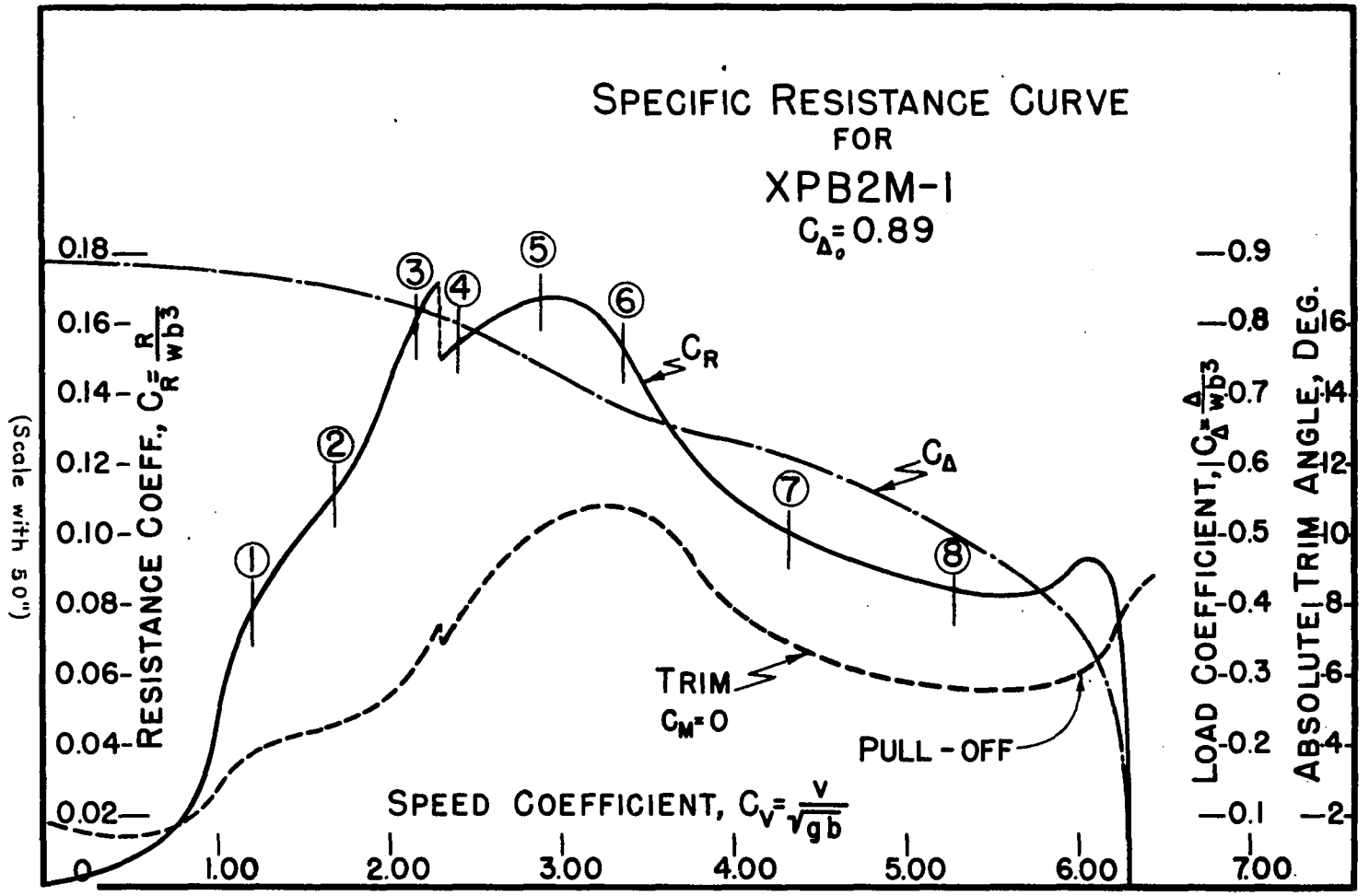

Figure 7.- This chart shows a specific resistance curve constructed from the two charts opposite, for the indicated curves of C_Δ and τ. The numbers in the circles on this chart are from the locations indicated by the same numbers on the opposite page, Fig. 8.

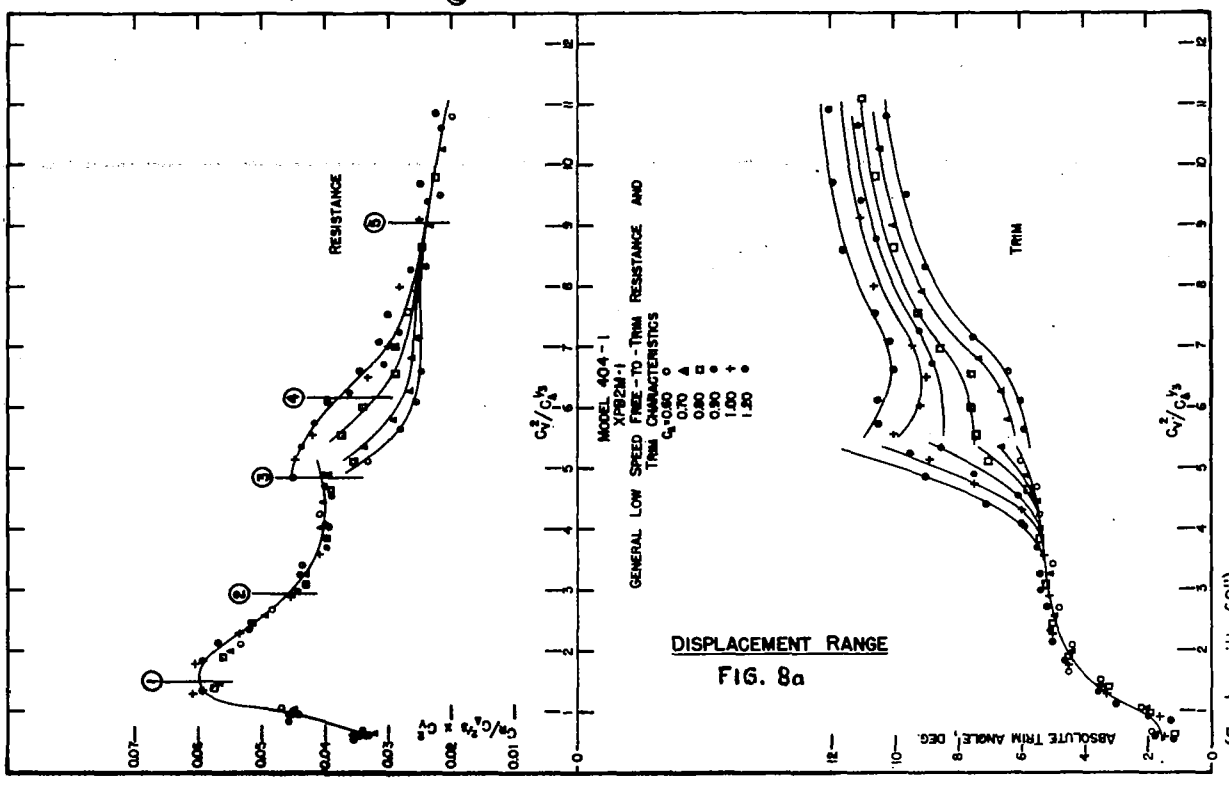

DISPLACEMENT RANGE

FIG. 8a

XPB2M-1

STABILITY, RESISTANCE AND MOMENT CHARACTERISTICS FROM GENERAL TESTS

STEVENS MODELS NO. 339-1 AND 404-1

C.G. = 0.43 b fwd of step, 0.90 b above B.L.

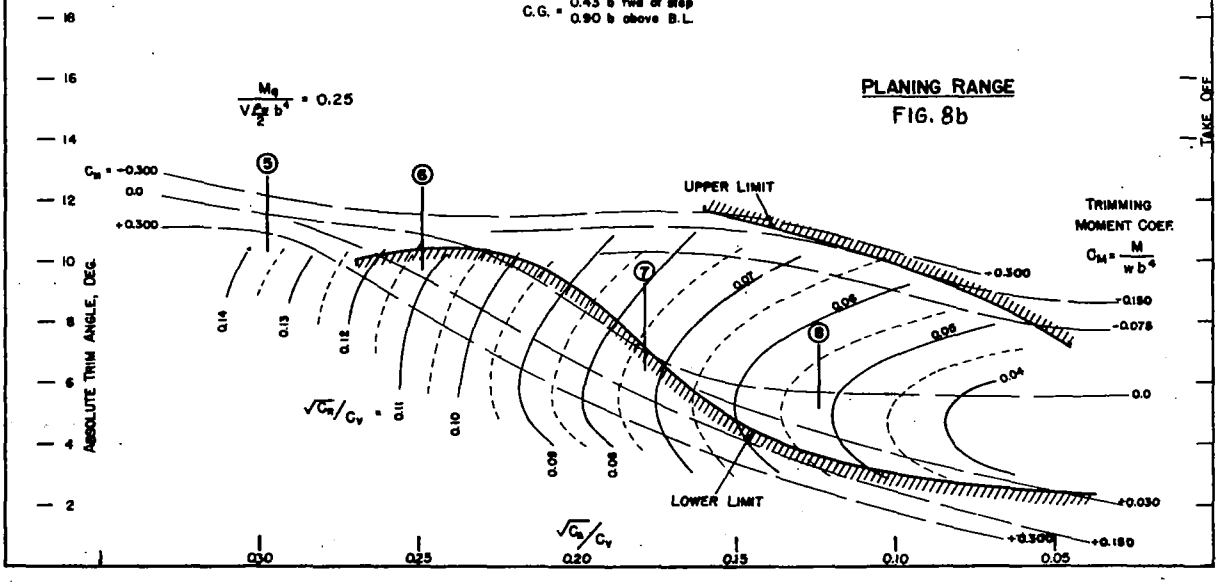

PLANING RANGE

FIG. 8b

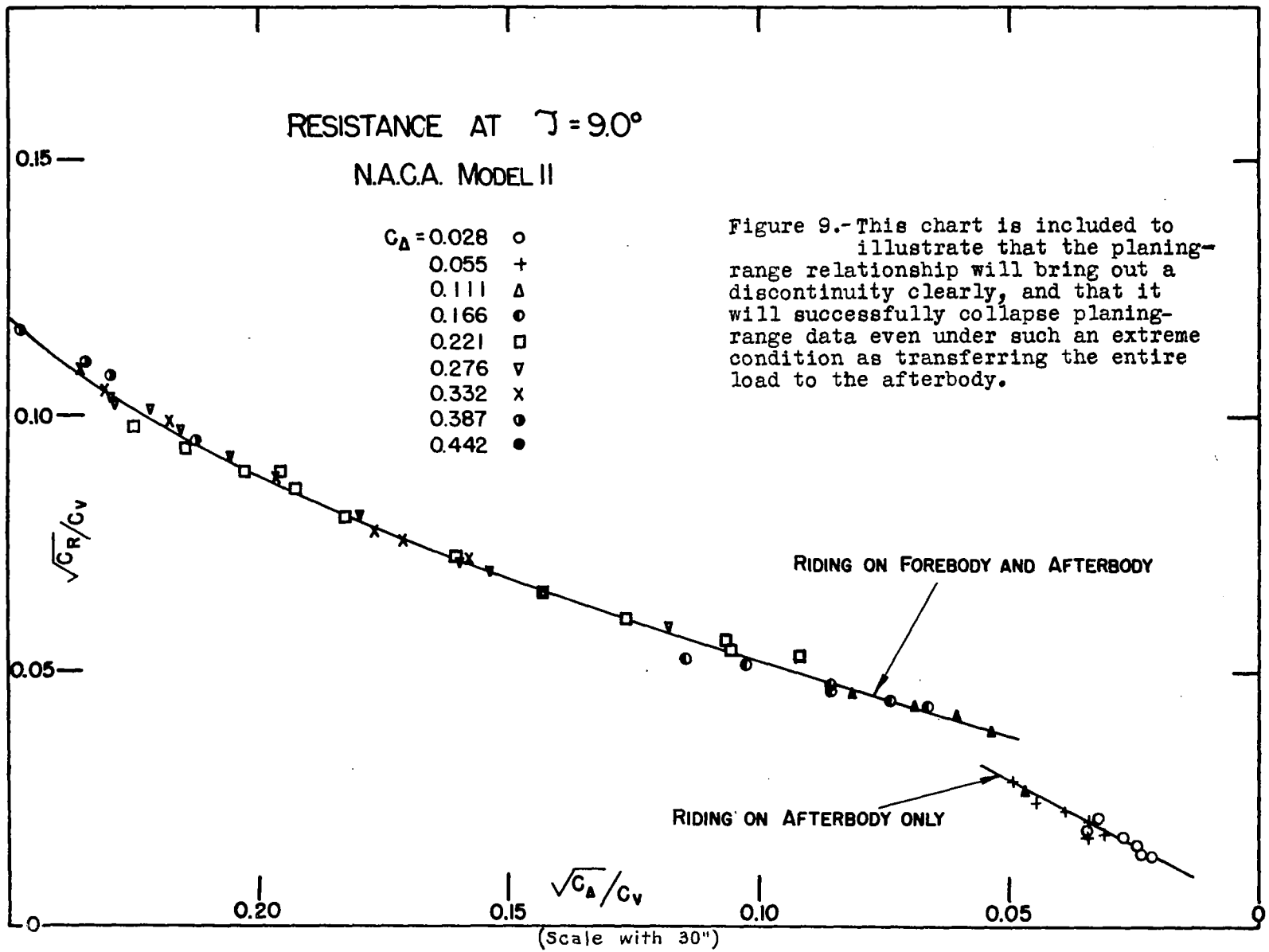

Figure 9.- This chart is included to illustrate that the planing-range relationship will bring out a discontinuity clearly, and that it will successfully collapse planing-range data even under such an extreme condition as transferring the entire load to the afterbody.